

Modeling the resonance $T_{cs0}^a(2900)^{++}$ as a hadronic molecule $D^{*+}K^{*+}$

S. S. Agaev,¹ K. Azizi,^{2,3} and H. Sundu^{4,5}

¹*Institute for Physical Problems, Baku State University, Az-1148 Baku, Azerbaijan*

²*Department of Physics, University of Tehran, North Karegar Avenue, Tehran 14395-547, Iran*

³*Department of Physics, Doğuş University, Dudullu-Ümraniye, 34775 Istanbul, Türkiye*

⁴*Department of Physics, Kocaeli University, 41380 Izmit, Türkiye*

⁵*Department of Physics Engineering, Istanbul Medeniyet University, 34700 Istanbul, Türkiye*

(ΩDated: April 26, 2023)

The doubly charged scalar resonance $T_{cs0}^a(2900)^{++}$ is studied in the context of the hadronic molecule model. We consider $T_{cs0}^a(2900)^{++}$ as a molecule $M = D^{*+}K^{*+}$ composed of vector mesons, and calculate its mass, current coupling and full width. The spectroscopic parameters of M , i.e., its mass and current coupling, are found by means of the QCD two-point sum rule method by taking into account vacuum expectation values of quark, gluon and mixed operators up to dimension 10. The width of the molecule M is evaluated through the calculations of the partial widths of the decay channels $M \rightarrow D_s^+ \pi^+$, $M \rightarrow D_s^{*+} \rho^+$, and $M \rightarrow D^{*+} K^{*+}$. Partial widths of these processes are determined by strong couplings g_1 , g_2 , and g_3 of particles at vertices $MD_s^+ \pi^+$, $MD_s^{*+} \rho^+$, and $MD^{*+} K^{*+}$, respectively. We calculate the couplings g_i by employing the QCD light-cone sum rule approach and technical tools of the soft-meson approximation. Predictions obtained for the mass $m = (2924 \pm 107)$ MeV and width $\Gamma = (123 \pm 25)$ MeV of the hadronic molecule M allow us to consider it as a possible candidate of the resonance $T_{cs0}^a(2900)^{++}$.

I. INTRODUCTION

Recently, the LHCb collaboration discovered new resonances $T_{cs0}^a(2900)^{0/++}$ (in what follows, $T_{cs0}^{a0/++}$) in the processes $B^0 \rightarrow \bar{D}^0 D_s^+ \pi^-$ and $B^+ \rightarrow D^- D_s^+ \pi^+$ [1, 2], respectively. They were fixed in the $D_s^+ \pi^-$ and $D_s^+ \pi^+$ mass distributions, and are structures with spin-parity $J^P = 0^+$. From the analysis of the decay channels of $T_{cs0}^{a0/++}$ it becomes clear that they are fully open flavor four-quark systems of $cd\bar{s}\bar{u}/cu\bar{s}\bar{d}$. Their resonant parameters are consistent with each other, which means that they are members of an isospin triplet: This is the first observation of an isospin triplet of exotic mesons with four different quark flavors. The resonance T_{cs0}^{a++} has an additional attractive feature as the first doubly charged exotic meson discovered experimentally.

It should be emphasized that $T_{cs0}^{a0/++}$ are not first fully open flavor resonances seen by the LHCb experiment. Indeed, previously LHCb informed about scalar $X_0(2900)$ and vector $X_1(2900)$ structures (hereafter X_0 and X_1 , respectively), which were found in the $D^- K^+$ invariant mass distribution of the decay $B^+ \rightarrow D^+ D^- K^+$ [3, 4]. In a four-quark picture both X_0 and X_1 have the same contents $ud\bar{s}\bar{c}$. New resonances $T_{cs0}^{a0/++}$ fill up the list of such particles.

The exotic mesons built of four different quarks have already attracted the interest of researches. Relevant activities started from announcement by the $D0$ collaboration about the resonance $X(5568)$ [5, 6] presumably composed of quarks $sub\bar{d}$. Despite the fact that LHCb, CMS and ATLAS experiments did not confirm existence of this state, technical tools elaborated during this activity led to some interesting results, and are still in use in numerous research works. One of such results is prediction of a charmed partner $X_c = [su][\bar{c}\bar{d}]$ of

$X(5568)$ in the diquark-antidiquark model [7, 8]. In our paper [7] it was investigated in a rather detailed form. Thus, we calculated the mass and full width of this tetraquark in the context of QCD sum rule method using different interpolating currents. In the case of scalar-scalar current we obtained $m_S = (2634 \pm 62)$ MeV and $\Gamma_S = (57.7 \pm 11.6)$ MeV, whereas the axial-axial current led to predictions $m_A = (2590 \pm 60)$ MeV and $\Gamma_A = (63.4 \pm 14.2)$ MeV. It is worth noting that an estimation (2.55 ± 0.09) GeV for the mass of X_c was made in Ref. [8], as well.

The doubly charged exotic mesons were also objects of interesting analyses. The $-2|e|$ charged scalar, pseudoscalar and axial-vector diquark-antidiquarks $Z_{\bar{c}s} = [sd][\bar{u}\bar{c}]$ were explored in Ref. [9]. Another class of tetraquarks $Z^{++} = [cu][\bar{s}\bar{d}]$ with the electric charge $2|e|$ are antiparticles of the states $Z_{\bar{c}s}$ and have the same masses and decay widths. Parameters of the vector tetraquark Z_V^{++} from this group of particles were found in Ref. [10].

The discovery of the resonances X_0 and X_1 highly intensified investigations of fully open flavor structures [11–33]. In these articles different models were suggested to explain the observed parameters of these states and understand their inner organizations. Traditionally they were explored in the diquark-antidiquark and hadronic molecule pictures, which are dominant models to account for similar experimental data. Thus, X_0 was treated as a scalar diquark-antidiquark state $[sc][\bar{u}\bar{d}]$ in Refs. [11, 12]. The X_0 was assigned to be the S -wave hadronic molecule $D^* K^{*+}$, whereas X_1 was examined as the P -wave diquark-antidiquark state $[ud][\bar{c}\bar{s}]$ in Ref. [13]. There were attempts to consider these structures as rescattering effects. In fact, in Ref. [15] it was asserted that two resonance-like peaks in the process $B^+ \rightarrow D^+ D^- K^+$ may be generated by rescattering ef-

fects and occur in the LHCb experiment as the states X_0 and X_1 .

The structures X_0 and X_1 were studied in our publications as well. The mass and width of the resonance X_0 were calculated in Ref. [34] in the framework of a hadronic molecule model $\overline{D}^{*0}K^{*0}$. Results found in this work for the parameters of X_0 allowed us to confirm its molecule nature. We explored also the resonance X_1 by considering it as a vector diquark-antidiquark state $X_V = [ud][\overline{c}\overline{s}]$ [35]: It turned out that the diquark-antidiquark structure is an appropriate model to explain the measured parameters of X_1 .

The LHCb observed only the vector tetraquark $X_V = [ud][\overline{c}\overline{s}]$, which was interpreted as X_1 . It is quite possible that, in near future, the diquark-antidiquark structures $[ud][\overline{c}\overline{s}]$ with other quantum numbers will be seen in various exclusive processes. Therefore, parameters of these yet hypothetical exotic mesons are necessary to form a theoretical basis for upcoming experimental activities. Motivated by this reason, we computed the masses and full widths of the ground-state and radially excited scalar particles $X_0^{(\prime)} = [ud][\overline{c}\overline{s}]$ [36]. The axial-vector and pseudoscalar tetraquarks X_{AV} and X_{PS} were investigated in Ref. [37], in which we evaluated their spectroscopic parameters, i.e., their masses and current couplings, and widths.

The resonances $T_{cs0}^{a0/++}$ are last experimentally confirmed members of fully open flavor tetraquark family. In this article we are going to study the doubly charged state T_{cs0}^{a++} , therefore, below, write down its parameters measured by LHCb [2]:

$$\begin{aligned} M_{\text{exp}} &= (2921 \pm 17 \pm 20) \text{ MeV}, \\ \Gamma_{\text{exp}} &= (137 \pm 32 \pm 17) \text{ MeV}. \end{aligned} \quad (1)$$

Observation of new tetraquarks $T_{cs0}^{a0/++}$ generated theoretical investigations aimed to bring them under one of existing models of four-quark mesons. In our article [38], we argued that diquark-antidiquark structures are not suitable for these resonances, because parameters of such states were already evaluated and predictions obtained for their masses are well below the LHCb data. One of possible ways to explain $T_{cs0}^{a0/++}$ is to treat them as hadronic molecules. Then T_{cs0}^{a++} may be interpreted as a hadronic molecule $D_s^{*+}\rho^+$ or $D^{*+}K^{*+}$. In Ref. [38], we realized first of these scenarios, and estimated the mass of molecule $D_s^{*+}\rho^+$ by employing the QCD two-point sum rule approach. Our result $m = (2917 \pm 135) \text{ MeV}$ for the mass of the molecule $D_s^{*+}\rho^+$ is consistent with Eq. (1).

The resonances $T_{cs0}^{a0/++}$ were investigated in Refs. [39–45] as well, in which authors used different models and calculational schemes. The one-boson exchange model was employed in Ref. [39] to study interactions in systems of $D^{(*)}K^{(*)}$ mesons. Analysis allowed the authors to assign T_{cs0}^{a++} to be an isovector $D^{*+}K^{*+}$ molecule state with the spin-parity $J^P = 0^+$ and mass 2891 MeV. Interpretation of new tetraquark candidate T_{cs0}^a as the resonance-like structure generated by threshold effects

was proposed in Ref. [40]. It was argued that the triangle singularity induced by the $\chi_{c1}K^*D^*$ loop peaks around the threshold D^*K^* and may simulate T_{cs0}^a . A multi-quark color flux-tube model was used to investigate the resonances $T_{cs0}^{a0/++}$ in the context of the diquark-antidiquark model [41]. The authors found that a system $[cu][\overline{s}\overline{d}]$ built of color antitriplet diquark and triplet antidiquark with the mass 2923 MeV is a very nice candidate to the resonance T_{cs0}^{a++} . Features of the charmed-strange tetraquarks were explored also in Ref. [43] in a nonrelativistic potential quark model. Decays of the neutral state T_{cs0}^{a0} in the molecular picture were considered in Ref. [44], whereas production mechanisms of the hidden- and open-charm tetraquarks in B decays were addressed in Ref. [45].

In the present work, we explore the resonance T_{cs0}^{a++} in the context of the hadronic molecule model. We implement the second scenario and model T_{cs0}^{a++} as the hadronic molecule $M = D^{*+}K^{*+}$. Our analyses of M include calculations of its mass m , current coupling f and full width Γ . The spectroscopic parameters of M are extracted from the QCD two-point sum rule computations [46, 47] by taking into account vacuum expectation values of different quark, gluon and mixed operators up to dimension 10.

To estimate the full width of the molecule M , we consider its decays to pairs of conventional mesons $D_s^+\pi^+$, $D_s^{*+}\rho^+$, and $D^{*+}K^{*+}$. Partial widths of these processes depend on parameters of initial and final-state particles, as well as on couplings g_i , which determine strong interactions of the molecule M and mesons at the vertices $MD_s^+\pi^+$, $MD_s^{*+}\rho^+$, and $MD^{*+}K^{*+}$, respectively. Because masses and decay constants of ordinary mesons are known, and spectroscopic parameters of M are object of present studies, only missed quantities are strong couplings g_i . The couplings g_i are evaluated in the framework of QCD light-cone sum rule (LCSR) method [48]. Additionally, to treat technical peculiarities of four-quark molecule-two conventional meson vertices, we invoke the technical methods of soft-meson approximation [49, 50].

This article is organized in the following way: In Sec. II, we find the sum rules for the mass m and current coupling f of the molecule $M = D^{*+}K^{*+}$ in the framework of QCD sum rule method. Numerical analysis of the quantities m and f is carried out in this section as well, where their values are evaluated. In section III, we investigate the vertices $MD_s^+\pi^+$, $MD_s^{*+}\rho^+$, and $MD^{*+}K^{*+}$ and calculate the corresponding strong couplings g_i , $i = 1, 2, 3$. Obtained information on g_i is used to find partial widths of these decay channels, and estimate full width of the molecule M . The section IV is reserved for our conclusions.

II. MASS m AND CURRENT COUPLING f OF THE HADRONIC MOLECULE $M = D^{*+}K^{*+}$

The key quantity necessary to investigate the spectroscopic parameters of the molecule M using the QCD two-point sum rule method, is the interpolating current $J(x)$ for this state. An analytic form of $J(x)$ depends on the structure and constituents of a four-quark exotic meson $\bar{q}_1\bar{q}_2q_3q_4$. In the molecule picture the color-singlet structures come from $[\mathbf{1}_c]_{\bar{q}_1q_3} \otimes [\mathbf{1}_c]_{\bar{q}_2q_4}$ and $[\mathbf{8}_c]_{\bar{q}_1q_3} \otimes [\mathbf{8}_c]_{\bar{q}_2q_4}$ and $(q_3 \leftrightarrow q_4)$ terms of the color group $SU_c(3)$. In the case under discussion, we assume that the hadronic molecule M is composed of two ordinary vector mesons D^{*+} and K^{*+} , and restrict our analysis by singlet-singlet type current. Then, in the $[\mathbf{1}_c]_{\bar{d}c} \otimes [\mathbf{1}_c]_{\bar{s}u}$ representation $J(x)$ takes the following form

$$J(x) = [\bar{d}_a(x)\gamma^\mu c_a(x)][\bar{s}_b(x)\gamma_\mu u_b(x)], \quad (2)$$

where a and b are color indices.

This current has the meson-meson structure and is a local product of two vector currents corresponding to the mesons D^{*+} and K^{*+} . It couples well to the molecule state $D^{*+}K^{*+}$. But, at the same time, $J(x)$ couples also to diquark-antidiquark states, because using Fierz transformation a molecule current can be presented as a weighted sum of different diquark-antidiquark currents [51]. In its turn, a diquark-antidiquark current is expressible via molecule structures (for instance, see Refs. [52, 53]). For example, the current $J(x)$ rewritten in the form

$$J(x) = \delta_{am}\delta_{bn}[\bar{d}_a\gamma^\mu c_m][\bar{s}_b\gamma_\mu u_n], \quad (3)$$

after Fierz transformation contains the vector-vector component

$$J_{VV} = -\frac{1}{2}\delta_{am}\delta_{bn}[\bar{d}_a\gamma^\mu u_n][\bar{s}_b\gamma_\mu c_m]. \quad (4)$$

Using the rearrangement of the color indices $\delta_{am}\delta_{bn} = \delta_{an}\delta_{bm} + \epsilon_{abk}\epsilon_{mnk}$, with ϵ_{ijk} being the Levi-Civita epsilon, it is not difficult to see that

$$J_{VV} = -\frac{1}{2}[\bar{d}_a\gamma^\mu u_a][\bar{s}_b\gamma_\mu c_b] + \dots \quad (5)$$

The term in Eq. (5) is the $-D_s^{*+}\rho^+/2$ meson-meson current, whereas dots indicate the second component which should be further manipulated to become diquark type current(s). In other words, $J(x)$ couples also to a molecule $D_s^{*+}\rho^+$ and can couple to other meson pairs such as $D_s^+\pi^+$ with the same contents and quantum numbers. Nevertheless, the current $J(x)$ corresponds mainly to the molecule $D^{*+}K^{*+}$, which will be demonstrated quantitatively in the next section by comparing its strong couplings g_i to different two-meson states.

The sum rules for the mass m and current coupling f of the hadronic molecule M can be obtained from analysis of the correlation function [46, 47],

$$\Pi(p) = i \int d^4x e^{ipx} \langle 0 | \mathcal{T} \{ J(x) J^\dagger(0) \} | 0 \rangle, \quad (6)$$

with \mathcal{T} being the time-ordering operator.

To derive the required sum rules, the correlator $\Pi(p)$ should be expressed using the physical parameters of the molecule M , as well as calculated in terms of the fundamental parameters of QCD in quark-gluon language. The first expression establishes the physical (phenomenological) side of the sum rules, for which we get

$$\Pi^{\text{Phys}}(p) = \frac{\langle 0 | J | M \rangle \langle M | J^\dagger | 0 \rangle}{m^2 - p^2} + \dots \quad (7)$$

To obtain $\Pi^{\text{Phys}}(p)$, we insert a complete set of the intermediate states with the content and quantum numbers of the state M into Eq. (6), and carry out integration over x . In Eq. (7), the contribution of the ground-state particle M is isolated and shown explicitly, whereas dots denote effects due to higher resonances and continuum states in the M channel.

For further simplification of $\Pi^{\text{Phys}}(p)$, it is convenient to introduce the physical parameters of M by means of the matrix element

$$\langle 0 | J | M \rangle = fm. \quad (8)$$

Then, we get the final formula for the function $\Pi^{\text{Phys}}(p)$:

$$\Pi^{\text{Phys}}(p) = \frac{f^2 m^2}{m^2 - p^2} + \dots \quad (9)$$

The r.h.s. of Eq. (9) contains only a trivial Lorentz structure, which is the unit matrix I. The function $f^2 m^2 / (m^2 - p^2)$ is the invariant amplitude $\Pi^{\text{Phys}}(p^2)$ that corresponds to this structure: It will be used in our following analysis.

The QCD side of the sum rules, $\Pi^{\text{OPE}}(p)$, has to be calculated in the operator product expansion (OPE) with some fixed accuracy. To derive $\Pi^{\text{OPE}}(p)$, we insert the interpolating current $J(x)$ into Eq. (6), contract the corresponding heavy and light quark fields, and write the obtained expression in terms of the corresponding quark propagators. Having carried out these manipulations, we get for $\Pi^{\text{OPE}}(p)$,

$$\begin{aligned} \Pi^{\text{OPE}}(p) &= i \int d^4x e^{ipx} \text{Tr} \left[\gamma_\mu S_c^{aa'}(x) \gamma_\nu S_d^{a'a}(-x) \right] \\ &\times \text{Tr} \left[\gamma^\mu S_u^{bb'}(x) \gamma^\nu S_s^{b'b}(-x) \right], \end{aligned} \quad (10)$$

where $S_c(x)$ and $S_{u(s,d)}(x)$ are the quark propagators. The explicit expressions of the heavy and light quarks propagators can be found in Ref. [54].

The correlator $\Pi^{\text{OPE}}(p)$ has also a simple structure $\sim I$ and is characterized by an amplitude $\Pi^{\text{OPE}}(p^2)$. To find a preliminary sum rule, we equate the amplitudes $\Pi^{\text{Phys}}(p^2)$ and $\Pi^{\text{OPE}}(p^2)$. This equality contains contributions coming from both the ground-state particle and higher resonances. The latter can be suppressed by applying the Borel transformation to both sides of the sum rule equality. Afterward, using the quark-hadron duality assumption, we subtract the suppressed terms from

the obtained expression. These manipulations lead to dependence of the sum rule equality on the Borel and continuum subtraction (threshold) parameters M^2 and s_0 . Obtained by this way, the expression and its derivative over $d/d(-1/M^2)$ allow us to find the sum rules for the mass m and coupling f of the molecule M , which read

$$m^2 = \frac{\Pi'(M^2, s_0)}{\Pi(M^2, s_0)}, \quad (11)$$

and

$$f^2 = \frac{e^{m^2/M^2}}{m^2} \Pi(M^2, s_0). \quad (12)$$

The function $\Pi(M^2, s_0)$ in Eqs. (11) and (12) is the invariant amplitude $\Pi^{\text{OPE}}(p^2)$ after the Borel transformation and continuum subtraction, and $\Pi'(M^2, s_0) = d\Pi(M^2, s_0)/d(-1/M^2)$.

The Borel transform of the amplitude $\Pi^{\text{Phys}}(p^2)$ is given by the formula

$$\mathcal{B}\Pi^{\text{Phys}}(p^2) = f m e^{-m^2/M^2}. \quad (13)$$

For the correlator $\Pi(M^2, s_0)$, we find a more complicated expression

$$\Pi(M^2, s_0) = \int_{\mathcal{M}^2}^{s_0} ds \rho^{\text{OPE}}(s) e^{-s/M^2} + \Pi(M^2), \quad (14)$$

where $\mathcal{M} = m_c + m_s$ is the mass of constituent quarks in the molecule M . It is worth noting, that we neglect masses of u and d quarks, but take into account terms $\sim m_s$. At the same time, we do not include into analysis contributions $\sim m_s^2$ and set $m_s^2 = 0$. The spectral density $\rho^{\text{OPE}}(s)$ is computed as an imaginary part of the amplitude $\Pi^{\text{OPE}}(p^2)$. Borel transforms some of terms obtained directly from $\Pi^{\text{OPE}}(p)$ are denoted in Eq. (14) by $\Pi(M^2)$. In this paper, calculations are carried out by taking into account vacuum condensates up to dimension 10. Analytical expressions of $\rho^{\text{OPE}}(s)$ and $\Pi(M^2)$ are lengthy, therefore we do not write down them here explicitly.

For numerical computations of m and f , one should specify different vacuum condensates, which enter to the sum rules in Eqs. (11) and (12). These condensates are universal parameters, which were extracted from analysis of numerous processes: Their numerical values are listed below:

$$\begin{aligned} \langle \bar{q}q \rangle &= -(0.24 \pm 0.01)^3 \text{ GeV}^3, \quad \langle \bar{s}s \rangle = (0.8 \pm 0.1) \langle \bar{q}q \rangle, \\ \langle \bar{q}g_s \sigma G q \rangle &= m_0^2 \langle \bar{q}q \rangle, \quad \langle \bar{s}g_s \sigma G s \rangle = m_0^2 \langle \bar{s}s \rangle, \\ m_0^2 &= (0.8 \pm 0.2) \text{ GeV}^2 \\ \langle \frac{\alpha_s G^2}{\pi} \rangle &= (0.012 \pm 0.004) \text{ GeV}^4, \\ \langle g_s^3 G^3 \rangle &= (0.57 \pm 0.29) \text{ GeV}^6, \\ m_s &= 93_{-5}^{+11} \text{ MeV}, \quad m_c = 1.27 \pm 0.02 \text{ GeV}. \end{aligned} \quad (15)$$

We have also included in Eq. (15) the masses of c and s quarks.

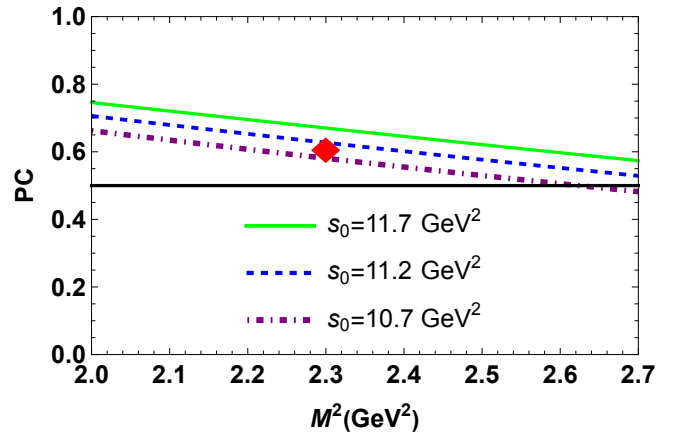


FIG. 1: Dependence of the pole contribution on the Borel parameter M^2 at fixed s_0 . The limit $\text{PC} = 0.5$ is shown by the horizontal black line. The red diamond notes the point, where the mass m of the molecule $M = D^{*+}K^{*+}$ has effectively been calculated.

The sum rules in Eqs. (11) and (12) depend also on the Borel and continuum threshold parameters M^2 and s_0 . The choice of working windows for M^2 and s_0 has to satisfy standard constraints imposed on the pole contribution (PC) and convergence of the operator product expansion. To quantify these constraints, it is appropriate to use expressions

$$\text{PC} = \frac{\Pi(M^2, s_0)}{\Pi(M^2, \infty)}, \quad (16)$$

and

$$R(M^2) = \frac{\Pi^{\text{DimN}}(M^2, s_0)}{\Pi(M^2, s_0)}, \quad (17)$$

where $\Pi^{\text{DimN}}(M^2, s_0) = \Pi^{\text{Dim}(8+9+10)}(M^2, s_0)$.

The PC is used to fix maximum of the Borel parameter M_{max}^2 , whereas its minimal value M_{min}^2 is limited by the convergence of OPE. In sum rule analyses of ordinary hadrons $\text{PC} \geq 0.5$ is a standard requirement. When studying multi-quark particles this constraint reduces the region of the allowed M^2 . To be convinced in convergence of the operator product expansion, we demand fulfillment of $R(M_{\text{min}}^2) \leq 0.05$.

Our calculations prove that the regions for the parameters M^2 and s_0 ,

$$M^2 \in [2, 2.7] \text{ GeV}^2, \quad s_0 \in [10.7, 11.7] \text{ GeV}^2, \quad (18)$$

meet all required restrictions. Thus, at $M^2 = 2.7 \text{ GeV}^2$ the pole contribution on average in s_0 is 0.53, whereas at $M^2 = 2 \text{ GeV}^2$ it equals to 0.72. In Fig. 1 the pole contribution is plotted as a function of M^2 at various fixed s_0 . It is seen that by excluding the small region $M^2 \geq 2.65 \text{ GeV}^2$ at $s_0 = 10.7 \text{ GeV}^2$ the pole contribution exceeds 0.5. On average in s_0 , the constraint $\text{PC} \geq 0.5$ is satisfied in the all working window for the Borel parameter. At the minimum point $M^2 = 2 \text{ GeV}^2$, we find

$R(2 \text{ GeV}^2) \approx 0.015$ and the sum of dimension-8, 9, 10 contributions is less than 1.5% of the full result.

Dominance of the perturbative contribution to $\Pi(M^2, s_0)$, and convergence of the operator product expansion are another important problems in the sum rule studies. In Fig. 2, we compare the perturbative and nonperturbative components of the correlation function. One sees that the perturbative contribution to $\Pi(M^2, s_0)$ prevails over nonperturbative one, and forms more than 53% of $\Pi(M^2, s_0)$ already at $M^2 = 2 \text{ GeV}^2$ growing gradually in the considered range of M^2 . From this figure it is also clear that convergence of OPE is satisfied: Contributions of the nonperturbative terms reduce by increasing the dimensions of the corresponding operators. There is some disordering in these contributions connected with smallness of gluon condensates. The dimension-3, 6, 9 and 10 terms are positive. The Dim3 and Dim6 contributions numerically exceed contributions of other operators, whereas Dim9 and Dim10 terms are very small and not shown in the plot.

Predictions for m and f are obtained by taking the mean values of these parameters calculated at different choices of M^2 and s_0 :

$$\begin{aligned} m &= (2924 \pm 107) \text{ MeV}, \\ f &= (4.3 \pm 0.7) \times 10^{-3} \text{ GeV}^4. \end{aligned} \quad (19)$$

The m and f from Eq. (19) effectively correspond to the

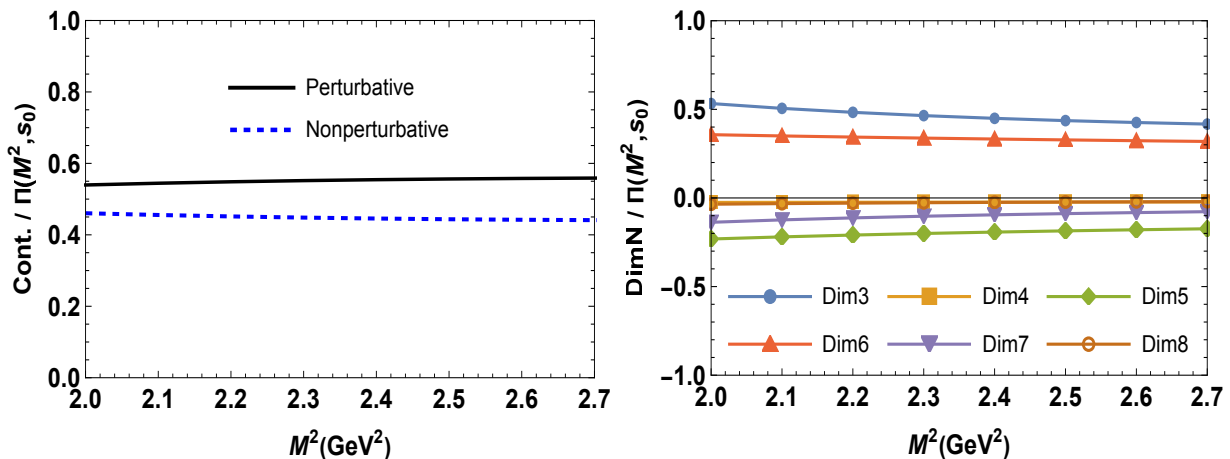


FIG. 2: Left: Different contributions to $\Pi(M^2, s_0)$ normalized to 1 as functions of the Borel parameter M^2 , Right: Normalized contributions of various operators to $\Pi(M^2, s_0)$ as functions of M^2 . All curves in this figure have been calculated at $s_0 = 11.2 \text{ GeV}^2$.

III. WIDTH OF THE MOLECULE M

The quark content, spin-parity and mass of the molecule $M = D^{*+}K^{*+}$ allow us to classify its decay

sum rules' results at $M^2 = 2.3 \text{ GeV}^2$ and $s_0 = 11.2 \text{ GeV}^2$ noted in Fig. 1 by the red diamond. This point is approximately at the middle of the intervals shown in Eq. (18), where the pole contribution is $\text{PC} \approx 0.62$. The circumstances discussed above ensure the ground-state nature of M and reliability of the obtained results.

The dependence of the mass m on the parameters M^2 and s_0 is drawn in Fig. 3. In general, a physical quantity should not depend on the auxiliary parameter of computations M^2 . Nevertheless, such residual dependence of m on the Borel parameter, as well as on s_0 exists and generates theoretical ambiguities of the extracted predictions in Eq. (19). It is worth noting that these ambiguities are smaller for m than for f . Indeed, for the mass they are equal only to $\pm 4\%$ of the central value, whereas in the case of f , they amount to $\pm 16\%$. Such difference is connected by the analytical forms of the sum rules for these quantities: The mass m is given by the ratio of the correlation functions which smooths relevant effect, whereas f depends on $\Pi(M^2, s_0)$ itself.

Our result for the mass of the molecule $D^{*+}K^{*+}$ agrees very well with the LHCb datum. This is necessary, but not enough to make credible conclusions about the nature of the resonance T_{cs0}^{a++} : For more reliable statements, one needs to estimate also the full width of the hadronic molecule $D^{*+}K^{*+}$ suggested in this paper to model T_{cs0}^{a++} .

channels. Because T_{cs0}^{a++} was seen in the $D_s^+ \pi^+$ invariant mass distribution, the process $M \rightarrow D_s^+ \pi^+$ should be the dominant decay channel of the molecule M . The processes $M \rightarrow D_s^{*+} \rho^+$ and $M \rightarrow D^{*+} K^{*+}$ are also among

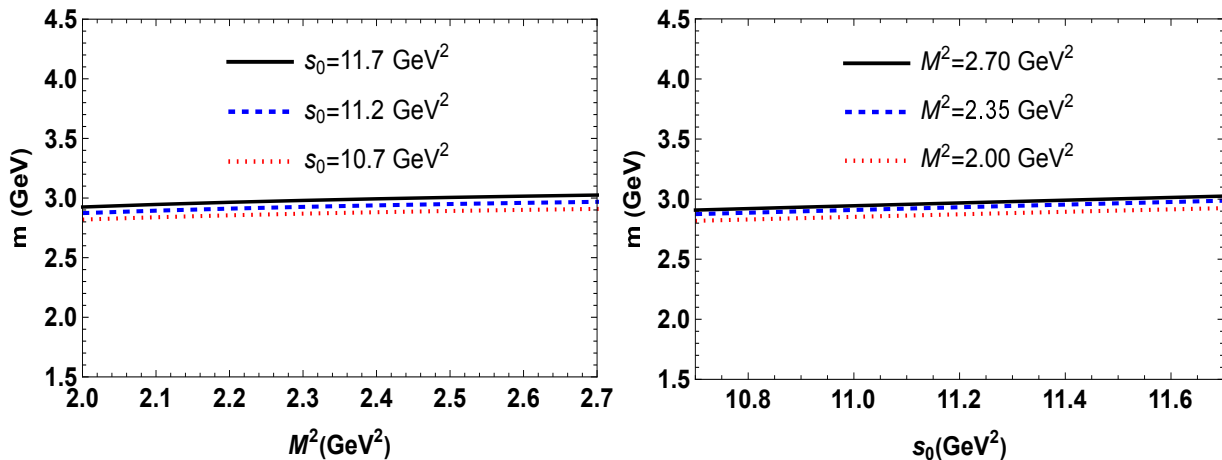


FIG. 3: Mass m of the molecule M as functions of the Borel M^2 (left panel), and continuum threshold s_0 parameters (right panel).

the kinematically allowed decay modes of the M . We are going to evaluate the full width of the molecule M using these decay channels. It is noting that, ρ^+ and K^{*+} mesons decay almost exclusively to $\pi^+\pi^0$ and $(K\pi)^+$ pairs (see, Ref. [55]), therefore widths of the last two processes can be considered also as widths of the modes $M \rightarrow D_s^{*+}\pi^+\pi^0$ and $M \rightarrow D^{*+}(K\pi)^+$, respectively.

Partial widths of aforementioned processes are determined by the strong couplings g_i at vertices $MD_s^+\pi^+$, and etc. One of the effective ways to evaluate them is the QCD light-cone sum rule method [48]. In this approach, the QCD side of the sum rule, instead of the local vacuum condensates, is expressed in terms of one of the final mesons' distribution amplitudes (DAs). In general, the DAs of a hadron are nonlocal matrix elements of various operators with different twists sandwiched between the hadron and vacuum states. They are specific for each particle and modeled by taking into account the available experimental data. The LCSR method is suitable for analysis of not only the conventional hadrons, but also the multi-quark systems such as tetraquarks, pentaquarks, etc. In the case of tetraquark-meson-meson vertices, however, these DAs reduce to the local matrix elements of the meson. For treatment of such vertices, one needs to apply some additional mathematical tools. The LCSR method was adapted for investigation of the tetraquark-meson-meson vertices in Ref. [56] and applied to study numerous decays of four-quark exotic mesons [54].

A. Decay $M \rightarrow D_s^+\pi^+$

Here, we consider, in a detailed manner, the decay of the molecule M to pair of pseudoscalar mesons $D_s^+\pi^+$. Partial width of this process depends on the spectroscopic parameters of the initial and final-state particles. The

spectroscopic parameters of M have been evaluated in the previous section. The masses and decay constants of the mesons D_s^+ and π^+ are available from other sources. The only unknown quantity required to calculate the $M \rightarrow D_s^+\pi^+$ decays's partial width is the strong coupling g_1 of the particles at the vertex $MD_s^+\pi^+$.

The coupling g_1 is defined in terms of the on-mass-shell matrix element,

$$\langle \pi(q)D_s(p) | M(p') \rangle = g_1 p \cdot p', \quad (20)$$

where the mesons π^+ and D_s^+ are denoted as π and D_s , respectively. In Eq. (20) p' , p and q are four-momenta of M , and mesons D_s and π .

In the framework of the LCSR method the sum rule for the coupling g_1 can be obtained from the correlation function,

$$\Pi(p, q) = i \int d^4x e^{ipx} \langle \pi(q) | \mathcal{T} \{ J^{D_s}(x) J^\dagger(0) \} | 0 \rangle, \quad (21)$$

where $J(x)$ is the current for the molecule M given by Eq. (2). The interpolating current $J^{D_s}(x)$ for the meson D_s^+ is defined by the formula

$$J^{D_s}(x) = \bar{s}_j(x) i \gamma_5 c_j(x), \quad (22)$$

with j being the color index.

At this stage of our analysis, we express the correlation function $\Pi(p, q)$ using the physical parameters of the particles involved into the decay process. To this end, we write $\Pi^{\text{Phys}}(p, q)$ in the factorized form [50, 57],

$$\begin{aligned} \Pi^{\text{Phys}}(p, q) &= \frac{\langle \pi(q)D_s(p) | M(p') \rangle \langle M(p') | J^\dagger | 0 \rangle}{(p'^2 - m^2)} \\ &\times \frac{\langle 0 | J^{D_s} | D_s(p) \rangle}{(p^2 - m_{D_s}^2)}, \end{aligned} \quad (23)$$

where m_{D_s} is the mass of the meson D_s^+ . As is seen, the function $\Pi^{\text{Phys}}(p, q)$ contains the matrix elements of the

vertex $MD_s^+\pi^+$, the molecule M and meson D_s^+ . The matrix element of M is known from Eq. (8), whereas for the meson D_s^+ we use

$$\langle 0|J^{D_s}|D_s(p)\rangle = \frac{f_{D_s}m_{D_s}^2}{m_c + m_s}, \quad (24)$$

with f_{D_s} being the decay constant of D_s^+ .

After simple manipulations, we get

$$\begin{aligned} \Pi^{\text{Phys}}(p, q) &= g_1 \frac{f_{D_s}m_{D_s}^2}{(m_c + m_s)(p^2 - m_{D_s}^2)} \\ &\times \frac{1}{(p'^2 - m^2)} p \cdot p' + \dots \end{aligned} \quad (25)$$

The term in Eq. (25) corresponds to the contribution of ground-state particles in M and D_s^+ channels. Effects of higher resonances and continuum states in these channels are denoted by ellipses. The function $\Pi^{\text{Phys}}(p, q)$ forms the physical side of the sum rule for the coupling g_1 . It has the Lorentz structure proportional to the unit matrix \mathbf{I} , therefore the expression in r.h.s. of Eq. (25) is the invariant amplitude $\Pi^{\text{Phys}}(p^2, p'^2)$, which depends on two variables p^2 and p'^2 .

The correlation function $\Pi(p, q)$ calculated in terms of quark propagators and matrix elements of the pion constitutes the QCD side of sum rules and is equal to

$$\begin{aligned} \Pi^{\text{OPE}}(p, q) &= - \int d^4x e^{ipx} [\gamma_\mu S_s^{bj}(-x) \gamma_5 S_c^{ja}(x) \gamma^\mu]_{\alpha\beta} \\ &\times \langle \pi(q) | \bar{u}_\alpha^b(0) d_\beta^a(0) | 0 \rangle, \end{aligned} \quad (26)$$

where α and β are the spinor indices.

The correlator $\Pi^{\text{OPE}}(p, q)$, apart from propagators of the c and s quarks, contains also the local matrix elements $\langle \pi | \bar{u}_\alpha^b d_\beta^a | 0 \rangle$ of the pion. In the standard LCSR method, while studying vertices of conventional mesons, the correlator depends on the nonlocal matrix elements of the meson (for instance, π meson), which after some transformations can be expressed in terms of its different DAs. In the case under discussion, the $\Pi^{\text{OPE}}(p, q)$ contains the pion's local matrix elements appearance of which has a simple explanation. Indeed, because the hadronic molecule M is built of four valence quarks located at space-time position $x = 0$, contractions of two quark operators from the currents $J^{D_s}(x)$ and $J(x)$ leave free the two quark fields from M at the same position $x = 0$. This feature of the correlation function $\Pi^{\text{OPE}}(p, q)$ connected with differences in the quark contents of tetraquarks and ordinary mesons is unavoidable effect for all tetraquark-meson-meson vertices.

It turns out that the $\Pi^{\text{OPE}}(p, q)$ -type correlators emerge in the limit $q \rightarrow 0$ in LCSR calculations [50], which is known as the soft-meson approximation. In this approximation, $p = p'$ and invariant amplitudes $\Pi^{\text{Phys}}(p^2)$ and $\Pi^{\text{OPE}}(p^2)$ depend only on one variable p^2 . It is worth emphasizing that the limit $q \rightarrow 0$ is applied to hard parts of the invariant amplitudes, whereas in their

soft parts (i.e., in matrix elements) terms $\sim q^2 = m^2$ are taken into account. In other words, soft-meson approximation should not be considered as a massless limit of the correlation functions.

Technical difficulties generated by this limit in the physical side of sum rules can be cured by means of technical tools elaborated in Refs. [49, 50]. It is important that the sum rules for the strong couplings obtained using the full LCSR method, and soft-meson approximation lead to numerically close results [50]. To clarify this last point, we note that in the full version of the LCSR method a sum rule for the strong coupling at a vertex of three conventional mesons depends on numerous two- and three-particle quark-gluon DAs of a final meson. In the limit $q \rightarrow 0$ in this expression survive only a few leading terms. Because their contributions are numerically decisive, for the strong coupling the full version and soft-meson limit of the light-cone sum rules give close predictions. Thus, in Ref. [50] the couplings $g_{D^*D\pi}$ and $g_{B^*B\pi}$ at the vertices $D^*D\pi$ and $B^*B\pi$ were calculated using both of these methods. In the full LCSR approach these couplings are equal to

$$g_{D^*D\pi}^{\text{full}} = 12.5 \pm 1.0, \quad g_{B^*B\pi}^{\text{full}} = 29 \pm 3, \quad (27)$$

whereas in the soft-meson approximation, the authors found

$$g_{D^*D\pi}^{\text{soft}} = 11 \pm 2, \quad g_{B^*B\pi}^{\text{soft}} = 28 \pm 6. \quad (28)$$

As is seen, values of the couplings are very close to each other, though uncertainties in the soft-limit are larger than in the full version [50].

These arguments do not imply a necessity of the soft-meson approximation to study all of the vertices containing four-quark states. Two tetraquark-meson vertices, for example, can be readily investigated in the context of the conventional LCSR method [58].

The local matrix elements, $\langle \pi | \bar{u}_\alpha^b d_\beta^a | 0 \rangle$, carry color and spinor indices and are uneasy objects for further operations. We can rewrite them in convenient forms by expanding $\bar{u}d$ over the full set of Dirac matrices Γ^J ,

$$\Gamma^J = \mathbf{1}, \quad \gamma_5, \quad \gamma_\mu, \quad i\gamma_5\gamma_\mu, \quad \sigma_{\mu\nu}/\sqrt{2}, \quad (29)$$

and projecting onto the colorless states

$$\bar{u}_\alpha^b(0) d_\beta^a(0) \rightarrow \frac{1}{12} \delta^{ba} \Gamma_{\beta\alpha}^J [\bar{u}(0) \Gamma^J d(0)]. \quad (30)$$

The operators $\bar{u} \Gamma^J d$, sandwiched between the π meson and vacuum, generate local matrix elements of the π meson, which can be implemented into $\Pi^{\text{OPE}}(p, q)$.

The expression obtained for the $\Pi^{\text{OPE}}(p^2)$ in the soft limit is considerably more simple than the invariant amplitude in the full version of LCSR method. But, at the same time, soft-meson approximation produces problems in the physical side of the sum rule. Below, we will come back to finish calculation of $\Pi^{\text{OPE}}(p^2)$, but now it is time

to fix sources of complications in $\Pi^{\text{Phys}}(p^2, p'^2)$. To this end, we rewrite this amplitude in the soft limit

$$\Pi^{\text{Phys}}(p^2) = g_1 \frac{f m f_{D_s} m_{D_s}^2}{2(m_c + m_s)(p^2 - \tilde{m}^2)^2} \times (2\tilde{m}^2 - m_\pi^2) + \dots, \quad (31)$$

where $\tilde{m}^2 = (m^2 + m_{D_s}^2)/2$ and m_π is the mass of the pion. It is seen that the amplitude $\Pi^{\text{Phys}}(p^2)$, in the soft approximation, instead of two poles at different points has one double pole at $p^2 = \tilde{m}^2$.

The Borel transformation of $\Pi^{\text{Phys}}(p^2)$ is given by the expression,

$$\Pi^{\text{Phys}}(M^2) = \left[g_1 \frac{f m f_{D_s} m_{D_s}^2}{2(m_c + m_s)} (2\tilde{m}^2 - m_\pi^2) + AM^2 \right] \frac{e^{-\tilde{m}^2/M^2}}{M^2} + \dots. \quad (32)$$

Apart from the ground-state contribution, in the soft limit, the amplitude $\Pi^{\text{Phys}}(M^2)$ contains additional unsuppressed terms $\sim A$ [50]. These terms correspond to the transitions from the excited states in $M = D^{*+}K^{*+}$ channel with $m^* > m$, and are not suppressed relative to the ground-state contribution even after the Borel transformation. These circumstances make problematic extraction of the g_1 from Eq. (32). The contributions $\sim A$ can be removed from the physical side of the sum rule by means of the operator $\mathcal{P}(M^2, \tilde{m}^2)$ [49, 50],

$$\mathcal{P}(M^2, \tilde{m}^2) = \left(1 - M^2 \frac{d}{dM^2} \right) M^2 e^{\tilde{m}^2/M^2}, \quad (33)$$

which should be applied to both sides of the sum rule equality.

After this operation the remaining suppressed terms in $\Pi^{\text{Phys}}(M^2)$, denoted in Eq. (32) by ellipses, can be subtracted by a standard way. As a result, we find the sum rule for the strong coupling g_1 , which reads

$$g_1 = \frac{2(m_c + m_s)}{f m f_{D_s} m_{D_s}^2 (2\tilde{m}^2 - m_\pi^2)} \mathcal{P}(M^2, \tilde{m}^2) \Pi^{\text{OPE}}(M^2, s_0), \quad (34)$$

where $\Pi^{\text{OPE}}(M^2, s_0)$ is the Borel transformed and subtracted invariant amplitude $\Pi^{\text{OPE}}(p^2)$.

Recipes to compute the correlation function $\Pi^{\text{OPE}}(p, q)$ in the soft approximation were explained in Ref. [56], therefore we give only principal points of these calculations. Thus, having substituted the expansion (30) into Eq. (26), we perform summations over color indices and fix the local matrix elements of the pion that contribute to the $\Pi^{\text{OPE}}(p, q)$ in the soft-meson limit. It turns out that the contributions to $\Pi^{\text{OPE}}(p, q = 0)$ come from the pion's two-particle twist-3 matrix element,

$$\langle 0 | \bar{d} i \gamma_5 u | \pi \rangle = f_\pi \mu_\pi, \quad (35)$$

where

$$\mu_\pi = \frac{m_\pi^2}{m_u + m_d} = -\frac{2\langle \bar{q}q \rangle}{f_\pi^2}. \quad (36)$$

Parameters	Values (in MeV units)
m_{D_s}	1969.0 ± 1.4
m_π	139.57039 ± 0.00017
$m_{D_s^*}$	2112.2 ± 0.4
m_ρ	775.11 ± 0.34
m_{D^*}	2010.26 ± 0.05
m_{K^*}	891.67 ± 0.26
f_{D_s}	249.9 ± 0.5
f_π	130.2 ± 0.8
$f_{D_s^*}$	268.8 ± 6.5
f_ρ	216 ± 3
f_{D^*}	223.5 ± 0.5
f_{K^*}	204 ± 0.3

TABLE I: Masses and decay constants of the mesons $D_s^{(*)}$, D^* , K^* , π and ρ , which have been used in numerical computations.

The second equality in Eq. (36) arises from the partial conservation of axial-vector current (PCAC).

The amplitude $\Pi^{\text{OPE}}(M^2, s_0)$ is given by the formula

$$\Pi^{\text{OPE}}(M^2, s_0) = \frac{f_\pi \mu_\pi}{8\pi^2} \int_{\mathcal{M}^2}^{s_0} \frac{ds(m_c^2 - s)}{s} \times (m_c^2 - 2m_c m_s - s) e^{-s/M^2} + f_\pi \mu_\pi \Pi_{\text{NP}}(M^2). \quad (37)$$

The first term in Eq. (37) is the perturbative component of the $\Pi^{\text{OPE}}(M^2, s_0)$. The nonperturbative term $\Pi_{\text{NP}}(M^2)$ is computed with dimension-9 accuracy and has the following form:

$$\begin{aligned} \Pi_{\text{NP}}(M^2) = & \frac{\langle \bar{s}s \rangle}{6M^2} [M^2(2m_c - m_s) - m_c^2 m_s] e^{-m_c^2/M^2} \\ & + \langle \frac{\alpha_s G^2}{\pi} \rangle \frac{m_c}{72M^4} \int_0^1 \frac{dx}{(1-x)^3} [m_s(1-x)(2M^2 + m_c^2) \\ & - m_c^3 x] e^{-m_c^2/[M^2(1-x)]} - \frac{\langle \bar{s}g\sigma Gs \rangle m_c^3}{6M^6} (M^2 - m_c m_s) \\ & \times e^{-m_c^2/M^2} + \langle \frac{\alpha_s G^2}{\pi} \rangle \langle \bar{s}s \rangle \frac{\pi^2 m_c}{9M^8} [M^2 m_c (m_c + m_s) \\ & - 2m_c^3 m_s - M^4] e^{-m_c^2/M^2} + \langle \frac{\alpha_s G^2}{\pi} \rangle \langle \bar{s}g\sigma Gs \rangle \frac{\pi^2 m_c}{18M^{12}} \\ & \times [3M^6 - 20m_c^5 m_s + 10m_c^3 M^2 (m_c + 2m_s) \\ & - 4M^4 m_c (3m_c + m_s)] e^{-m_c^2/M^2}. \end{aligned} \quad (38)$$

Besides the vacuum condensates, the sum rule in Eq. (34) contains also the masses and decay constants of the final-state mesons D_s^+ and π^+ . Numerical values of these parameters, as well as parameters of other mesons, which will be necessary later, are presented in Table I. For the decay constants of the mesons D_s^{*+} and D^{*+} , we employ predictions of the QCD lattice method [59]. For all other parameters, we use information of the Particle Data Group, mainly its last edition Ref. [55]. All these

input parameters were either measured experimentally or extracted by means of alternative theoretical approaches.

Numerical analysis demonstrates that the working regions shown in Eq. (18) used in calculations of the M molecule's mass meet the required restrictions on the Borel and continuum subtraction parameters M^2 and s_0 imposed in the case of the decay process. Therefore, in computations of $\Pi^{\text{OPE}}(M^2, s_0)$ the parameters M^2 and s_0 have been varied within the limits (18).

For g_1 , the numerical calculations yield

$$g_1 = (7.1 \pm 1.1) \times 10^{-1} \text{ GeV}^{-1}. \quad (39)$$

The partial width of the decay $M \rightarrow D_s^+ \pi^+$ is determined by the expression

$$\Gamma_1 [M \rightarrow D_s^+ \pi^+] = \frac{g_1^2 m_{D_s}^2}{8\pi} \lambda \left(1 + \frac{\lambda^2}{m_{D_s}^2} \right), \quad (40)$$

where $\lambda = \lambda(m, m_{D_s}, m_\pi)$ and

$$\lambda(a, b, c) = \frac{[a^4 + b^4 + c^4 - 2(a^2 b^2 + a^2 c^2 + b^2 c^2)]^{1/2}}{2a}. \quad (41)$$

Then it is not difficult to find that

$$\Gamma_1 [M \rightarrow D_s^+ \pi^+] = (71 \pm 23) \text{ MeV}, \quad (42)$$

which is large enough to confirm dominant nature of this channel.

B. Processes $M \rightarrow D_s^{*+} \rho^+$ and $M \rightarrow D^{*+} K^{*+}$

These two processes differ from previous decay by a vector nature of produced mesons. This fact modifies matrix elements of the vertices and formulas for decay widths of the processes. We concentrate on analysis of the decay $M \rightarrow D_s^{*+} \rho^+$, and write down only the final predictions for $M \rightarrow D^{*+} K^{*+}$.

The correlation function, which should be studied in the case of the decay $M \rightarrow D_s^{*+} \rho^+$, has the following form

$$\Pi_\mu(p, q) = i \int d^4 x e^{ipx} \langle \rho(q) | \mathcal{T} \{ J_\mu^{D_s^*}(x) J^\dagger(0) \} | 0 \rangle, \quad (43)$$

where $J_\mu^{D_s^*}(x)$ is the interpolating current for the meson D_s^{*+}

$$J_\mu^{D_s^*}(x) = \bar{s}_i(x) \gamma_\mu c_i(x). \quad (44)$$

The correlation function $\Pi_\mu(p, q)$ written down in terms of the matrix elements of the particles and the vertex $M D_s^{*+} \rho^+$ is given by the expression

$$\begin{aligned} \Pi_\mu^{\text{Phys}}(p, q) &= \frac{\langle \rho(q, \epsilon) D_s^{*+}(p, \epsilon) | M(p') \rangle \langle M(p') | J^\dagger | 0 \rangle}{(p'^2 - m^2)} \\ &\times \frac{\langle 0 | J_\mu^{D_s^*} | D_s^{*+}(p, \epsilon) \rangle}{(p^2 - m_{D_s}^2)} + \dots, \end{aligned} \quad (45)$$

where $m_{D_s^*}$ and ε_μ are the mass and polarization vector of the meson D_s^{*+} , and ϵ_ν is polarization vector of the ρ meson. The expression in Eq. (45) is the contribution of the ground-state particles to the physical side of the sum rule, whereas ellipses stand for the contributions of higher resonances and continuum states.

We introduce the matrix element of the meson D_s^{*+} by the formula

$$\langle 0 | J_\mu^{D_s^*} | D_s^{*+}(p, \varepsilon) \rangle = m_{D_s^*} f_{D_s^*} \varepsilon_\mu. \quad (46)$$

We also model the mass-shell matrix element of the vertex $M D_s^{*+} \rho^+$ in the following way:

$$\begin{aligned} \langle \rho(q, \epsilon) D_s^{*+}(p, \varepsilon) | M(p') \rangle &= g_2 [(q \cdot p) (\epsilon \cdot \varepsilon^*) \\ &- (p \cdot \epsilon) (q \cdot \varepsilon^*)], \end{aligned} \quad (47)$$

Then, it is not difficult to calculate the function $\Pi_\mu^{\text{Phys}}(p, q)$,

$$\begin{aligned} \Pi_\mu^{\text{Phys}}(p, q) &= \frac{f m m_{D_s^*} f_{D_s^*}}{(p'^2 - m^2)(p^2 - m_{D_s^*}^2)} \\ &\times \left(\frac{m_\rho^2 + m_{D_s^*}^2 - m^2}{2} \epsilon_\mu + p \cdot \epsilon q_\mu \right) + \dots, \end{aligned} \quad (48)$$

As is seen, $\Pi_\mu^{\text{Phys}}(p, q)$ contains two structures proportional to ϵ_μ and q_μ . We are going to employ the structure $\sim \epsilon_\mu$, and corresponding invariant amplitude which in the soft limit has the form

$$\widehat{\Pi}^{\text{Phys}}(p^2) = \frac{f m m_{D_s^*} f_{D_s^*}}{(p^2 - \widehat{m}^2)^2} \frac{m_\rho^2 + m_{D_s^*}^2 - m^2}{2}, \quad (49)$$

with \widehat{m}^2 being equal to $(m^2 + m_{D_s^*}^2)/2$.

The QCD side of the sum rule is determined by the correlator

$$\begin{aligned} \Pi_\mu^{\text{OPE}}(p, q) &= i \int d^4 x e^{ipx} [\gamma_\nu S_s^{bi}(-x) \gamma_\mu S_c^{ia}(x) \gamma^\nu]_{\alpha\beta} \\ &\times \langle \rho(q) | \bar{u}_\alpha^b(0) d_\beta^a(0) | 0 \rangle. \end{aligned} \quad (50)$$

This function has the same Lorentz structures as $\Pi_\mu^{\text{Phys}}(p, q)$. In the soft-meson approximation, it receives contribution from the matrix element

$$\langle 0 | \bar{d} \gamma_\nu u | \rho \rangle = f_\rho m_\rho \epsilon_\nu, \quad (51)$$

where f_ρ is the decay constant of the ρ meson.

Having fixed an amplitude which is proportional to ϵ_μ and labeled it by $\widehat{\Pi}^{\text{OPE}}(p^2)$ it is not difficult to write the sum rule for the strong coupling g_2

$$g_2 = \frac{2\mathcal{P}(M^2, \widehat{m}^2) \widehat{\Pi}^{\text{OPE}}(M^2, s_0)}{f m m_{D_s^*} f_{D_s^*} (m_\rho^2 + m_{D_s^*}^2 - m^2)}. \quad (52)$$

Here, $\widehat{\Pi}^{\text{OPE}}(M^2, s_0)$ is the amplitude $\widehat{\Pi}^{\text{OPE}}(p^2)$ after the Borel transformation and continuum subtraction

procedures. It does not differ considerably from the $\Pi^{\text{OPE}}(M^2, s_0)$ and has the following form

$$\begin{aligned} \widehat{\Pi}^{\text{OPE}}(M^2, s_0) &= \frac{f_\rho m_\rho}{48\pi^2} \int_{\mathcal{M}^2}^{s_0} \frac{ds(m_c^2 - s)}{s^2} \\ &\times (m_c^4 + m_c^2 m_s - 6m_c m_s s - 2s^2) e^{-s/M^2} \\ &+ f_\rho m_\rho \widehat{\Pi}_{\text{NP}}(M^2). \end{aligned} \quad (53)$$

The nonperturbative term $\widehat{\Pi}_{\text{NP}}(M^2)$ is given by the expression

$$\begin{aligned} \widehat{\Pi}_{\text{NP}}(M^2) &= \frac{\langle \bar{s}s \rangle m_c}{12M^2} (2M^2 - m_c m_s) e^{-m_c^2/M^2} \\ &+ \langle \frac{\alpha_s G^2}{\pi} \rangle \frac{m_c}{144M^4} \int_0^1 \frac{dx}{(1-x)^3} [m_c^3 x + (1-x)(m_c^2 m_s \\ &- 2m_s M^2 - m_c M^2)] e^{-m_c^2/[M^2(1-x)]} + \frac{\langle \bar{s}g\sigma Gs \rangle}{72M^6} \\ &\times (6m_c^4 m_s - 6m_c^3 M^2 - 2m_c^2 m_s M^2 - m_s M^4) e^{-m_c^2/M^2} \\ &+ \langle \frac{\alpha_s G^2}{\pi} \rangle \langle \bar{s}s \rangle \frac{\pi^2 m_c}{36M^8} [4m_c^3 m_s - 2M^2 m_c (m_c + 3m_s) \\ &+ 2M^4] e^{-m_c^2/M^2} + \langle \frac{\alpha_s G^2}{\pi} \rangle \langle \bar{s}g\sigma Gs \rangle \frac{\pi^2 m_c}{108M^{12}} \\ &\times [9M^6 - 60m_c^5 m_s + 10m_c^3 M^2 (3m_c + 7m_s) \\ &- 4M^4 m_c (9m_c + 4m_s)] e^{-m_c^2/M^2}. \end{aligned} \quad (54)$$

Numerical computations lead to the result

$$|g_2| = (9.8 \pm 1.2) \times 10^{-1} \text{ GeV}^{-1}. \quad (55)$$

The partial width of the decay $M \rightarrow D_s^{*+} \rho^+$ is determined by the formula

$$\Gamma_2 [M \rightarrow D_s^{*+} \rho^+] = \frac{|g_2|^2 m_\rho^2 \widehat{\lambda}}{8\pi} \left(3 + \frac{2\widehat{\lambda}^2}{m_\rho^2} \right), \quad (56)$$

where $\widehat{\lambda} = \lambda(m, m_{D_s^*}, m_\rho)$. Then, we get

$$\Gamma_2 [M \rightarrow D_s^{*+} \rho^+] = (15 \pm 4) \text{ MeV}. \quad (57)$$

The decay $M \rightarrow D^{*+} K^{*+}$ can be considered in a similar way. Omitting details, we write down predictions for the strong coupling g_3 and partial width of the process $M \rightarrow D^{*+} K^{*+}$:

$$g_3 = (1.5 \pm 0.3) \text{ GeV}^{-1}, \quad (58)$$

and

$$\Gamma_3 [M \rightarrow D^{*+} K^{*+}] = (37 \pm 10) \text{ MeV}. \quad (59)$$

Information gained in this section allows us to compare couplings of the current $J(x)$ to different two-meson states. It is seen that g_i corresponding to vertices $MD^{*+} K^{*+}$, $MD_s^{*+} \rho^+$ and $MD_s^+ \pi^+$ obey the inequalities $g_3 > |g_2| > g_1$. Hence, $J(x)$ describes mainly the

hadronic molecule $D^{*+} K^{*+}$, as it has been asserted in the Sec. II. Differences in the widths of relevant decays are connected not only with g_i , but generated also by λ -factors and parameters of produced mesons.

Using results obtained for the partial widths of the decays considered in this section, we can estimate the full width of the molecule M

$$\Gamma = (123 \pm 25) \text{ MeV}, \quad (60)$$

which should be confronted with the experimental data Eq. (1). It is seen that, although Γ and Γ_{exp} do not coincide, they are comparable with each other provided one takes into account errors of the measurements and theoretical analyses.

IV. CONCLUSIONS

In the present article, we have investigated features of the hadronic molecule $M = D^{*+} K^{*+}$, and calculated its mass and width. The mass of M has been computed using QCD two-point sum rule method. Prediction obtained for the mass $m = (2924 \pm 107) \text{ MeV}$ is in nice agreement with the LHCb datum for the mass of the resonance $T_{cs_0}^{a++}$. It also does not differ considerably from the mass $(2917 \pm 135) \text{ MeV}$ of the molecule $D_s^{*+} \rho^+$ suggested to model $T_{cs_0}^{a++}$ in our paper [38].

We have evaluated the width of the molecule M by calculating partial widths of the decay channels $M \rightarrow D_s^+ \pi^+$, $M \rightarrow D_s^{*+} \rho^+$, and $M \rightarrow D^{*+} K^{*+}$. To this end, we have found strong couplings of the particles at vertices $MD_s^+ \pi^+$, $MD_s^{*+} \rho^+$, and $MD^{*+} K^{*+}$ by means of QCD light-cone sum rule approach and soft-meson approximation. The strong coupling of the hadronic molecule M with final-state mesons is large in the case of mesons D^{*+} and K^{*+} , which is understandable because M is composed of these particles. Nevertheless, the partial width of the decay $M \rightarrow D^{*+} K^{*+}$ is less than that of the decay $M \rightarrow D_s^+ \pi^+$. The reason is that the kinematical factor λ in the expression of the decay widths in Eqs. (40) and (56) gets its largest value in the process $M \rightarrow D_s^+ \pi^+$. As a result, the dominant channel of M is the decay to a pair of the mesons D_s^+ and π^+ , which was actually observed by the LHCb collaboration.

The final result $\Gamma = (123 \pm 25) \text{ MeV}$ for the full width of the molecule M is compatible with the Γ_{exp} within the existing experimental and theoretical errors. The estimate for Γ may be further improved by taking into account another decay channels of the hadronic molecule M . It will be interesting also to compare the Γ and Γ_{exp} with predictions for the full width of the resonance $T_{cs_0}^{a++}$ obtained in the context of alternative methods. Nevertheless, based on our present results, we may consider the hadronic molecule $M = D^{*+} K^{*+}$ as a possible candidate to the doubly charged resonance $T_{cs_0}^{a++}$.

The isoscalar partner of $T_{cs_0}^{a++}$, namely the second resonance $T_{cs_0}^{a0}$ with quark content $cd\bar{s}\bar{u}$ may be modeled as a linear superposition of hadronic molecules $D^{*0}K^{*0}$ and $D_s^{*+}\rho^-$. The dominant decay channel of this state is the process $T_{cs_0}^{a0} \rightarrow D_s^+\pi^-$. The modes $T_{cs_0}^{a0} \rightarrow D^0K^0$, $D_s^{*+}\rho^-$ and $D^{*0}K^{*0}$ are other possible decay channels of $T_{cs_0}^{a0}$. Experimentally measured mass and width differences between $T_{cs_0}^{a++}$ and $T_{cs_0}^{a0}$ are equal to $\Delta m \approx 28$ MeV and $\Delta\Gamma \approx 15$ MeV, respectively. To be accepted as a reliable model for $T_{cs_0}^{a0}$ the molecule picture should be successfully confronted with the available data.

Another problem to be addressed here, is similarities and differences of the resonances $T_{cs_0}^{a0/++}$ and $X_{0(1)}$. It has been noted in Sec. I that $X_{0(1)}$ are exotic mesons composed of quarks $ud\bar{s}\bar{c}$. The scalar structures $T_{cs_0}^{a0}$ and X_0 differ from each other by quark-exchanges $\bar{u} \leftrightarrow u$ and $c \leftrightarrow \bar{c}$. They are neutral particles with masses 2892 MeV and 2866 MeV, respectively. It is seen, that a mass gap between these two structures is small. In Ref. [34], we modeled X_0 as a hadronic molecule $\bar{D}^{*0}K^{*0}$ and found its mass equal to 2868 MeV, which is in a very nice agree-

ment with the LHCb datum. The $\bar{D}^{*0}K^{*0}$ and a component $D^{*0}K^{*0}$ of the molecule model for $T_{cs_0}^{a0}$, have almost identical structures, therefore one expects the mass of the isoscalar state $T_{cs_0}^{a0}$ will be consistent with experiments.

The mass difference ~ 55 MeV between $T_{cs_0}^{a++}$ and X_0 is larger than the gap in the previous case which is connected presumably with doubly charged nature of $T_{cs_0}^{a++}$. We explored the vector resonance X_1 in Ref. [35] as a diquark-antidiquark state $[ud][\bar{c}\bar{s}]$ and achieved reasonable agreements with the LHCb data. In general, hadronic molecules composed of two mesons may be used to model vector particles as well. Because $T_{cs_0}^{a++}$ has the spin-parity $J^P = 0^+$, in this article, we have studied only scalar particle $D^{*+}K^{*+}$. Molecules with the same quark content but different spin-parities are yet hypothetical structures. They are interesting objects for theoretical researches as well, because may be discovered soon in various exclusive processes. Properties of the isoscalar resonance $T_{cs_0}^{a0}$, as well as counterparts of $T_{cs_0}^{a0/++}$ with different spin-parities are issues for future investigations.

-
- [1] [LHCb], arXiv:2212.02716 [hep-ex].
[2] [LHCb], arXiv:2212.02717 [hep-ex].
[3] R. Aaij *et al.* [LHCb], Phys. Rev. Lett. **125**, 242001 (2020).
[4] R. Aaij *et al.* [LHCb], Phys. Rev. D **102**, 112003 (2020).
[5] V. M. Abazov *et al.* [D0], Phys. Rev. Lett. **117**, 022003 (2017).
[6] V. M. Abazov *et al.* [D0], Phys. Rev. D **97**, 092004 (2018).
[7] S. S. Agaev, K. Azizi and H. Sundu, Phys. Rev. D **93**, 094006 (2016).
[8] W. Chen, H. X. Chen, X. Liu, T. G. Steele and S. L. Zhu, Phys. Rev. Lett. **117**, 022002 (2016).
[9] S. S. Agaev, K. Azizi and H. Sundu, Eur. Phys. J. C **78**, 141 (2018).
[10] S. S. Agaev, K. Azizi and H. Sundu, Phys. Lett. B **820**, 136530 (2021).
[11] M. Karliner and J. L. Rosner, Phys. Rev. D **102**, 094016 (2020).
[12] Z. G. Wang, Int. J. Mod. Phys. A **35**, 2050187 (2020).
[13] H. X. Chen, W. Chen, R. R. Dong and N. Su, Chin. Phys. Lett. **37**, 101201 (2020).
[14] M. Z. Liu, J. J. Xie and L. S. Geng, Phys. Rev. D **102**, 091502 (2020).
[15] X. H. Liu, M. J. Yan, H. W. Ke, G. Li and J. J. Xie, arXiv:2008.07190 [hep-ph].
[16] R. Molina and E. Oset, Phys. Lett. B **811**, 135870 (2020).
[17] M. W. Hu, X. Y. Lao, P. Ling and Q. Wang, Chin. Phys. C **45**, 021003 (2021).
[18] X. G. He, W. Wang and R. Zhu, Eur. Phys. J. C **80**, 1026 (2020).
[19] Q. F. Lu, D. Y. Chen and Y. B. Dong, Phys. Rev. D **102**, 074021 (2020).
[20] J. R. Zhang, Phys. Rev. D **103**, 054019 (2021).
[21] Y. Huang, J. X. Lu, J. J. Xie and L. S. Geng, Eur. Phys. J. C **80**, 973 (2020).
[22] Y. Xue, X. Jin, H. Huang and J. Ping, Phys. Rev. D **103**, 054010 (2021).
[23] G. Yang, J. Ping and J. Segovia, Phys. Rev. D **103**, 074011 (2021).
[24] T. W. Wu, Y. W. Pan, M. Z. Liu, S. Q. Luo, L. S. Geng, and X. Liu, Phys. Rev. D **105**, L031505 (2022).
[25] L. M. Abreu, Phys. Rev. D **103**, 036013 (2021).
[26] G. J. Wang, L. Meng, L. Y. Xiao, M. Oka and S. L. Zhu, Eur. Phys. J. C **81**, 188 (2021).
[27] C. J. Xiao, D. Y. Chen, Y. B. Dong and G. W. Meng, Phys. Rev. D **103**, 034004 (2021).
[28] X. K. Dong and B. S. Zou, Eur. Phys. J. A **57**, 139 (2021).
[29] T. J. Burns and E. S. Swanson, Phys. Rev. D **103**, 014004 (2021).
[30] A. E. Bondar and A. I. Milstein, JHEP **12**, 015 (2020).
[31] Y. K. Chen, J. J. Han, Q. F. Lü, J. P. Wang and F. S. Yu, Eur. Phys. J. C **81**, 71 (2021).
[32] R. M. Albuquerque, S. Narison, D. Rabetiarivony and G. Andriamanatrika, Nucl. Phys. A **1007**, 122113 (2021).
[33] B. Wang, and S. L. Zhu, Eur. Phys. J. C **82**, 419 (2022).
[34] S. S. Agaev, K. Azizi and H. Sundu, J. Phys. G **48**, 085012 (2021).
[35] S. S. Agaev, K. Azizi and H. Sundu, Nucl. Phys. A **1011**, 122202 (2021).
[36] S. S. Agaev, K. Azizi and H. Sundu, Phys. Rev. D **106**, 014019 (2022).
[37] H. Sundu, S. S. Agaev, and K. Azizi, Eur. Phys. J. C **83**, 198 (2023).
[38] S. S. Agaev, K. Azizi and H. Sundu, J. Phys. G to appear, arXiv:2207.02648 [hep-ph].
[39] R. Chen, and Q. Huang, arXiv:2208.10196 [hep-ph].
[40] Y. H. Ge, X. H. Liu, and H. W. Ke, Eur. Phys. J. C **82**, 955 (2022).
[41] J. Wei, Y. H. Wang, C. S. An, and C. R. Deng, Phys. Rev. D **106**, 096023 (2022).
[42] R. Molina, and E. Oset, Phys. Rev. D **107**, 056015

- (2023).
- [43] F. X. Liu, R. H. Ni, X. H. Zhong, and Q. Zhao, arXiv:2211.01711 [hep-ph].
- [44] Z. L. Yue, C. J. Xiao, and D. Y. Chen, arXiv:2212.03018 [hep-ph].
- [45] Q. Qin, J. L. Qui, and F. S. Yu, Eur. Phys. J. C **83**, 227 (2023).
- [46] M. A. Shifman, A. I. Vainshtein and V. I. Zakharov, Nucl. Phys. B **147**, 385 (1979).
- [47] M. A. Shifman, A. I. Vainshtein and V. I. Zakharov, Nucl. Phys. B **147**, 448 (1979).
- [48] I. I. Balitsky, V. M. Braun and A. V. Kolesnichenko, Nucl. Phys. B **312**, 509 (1989).
- [49] B. L. Ioffe and A. V. Smilga, Nucl. Phys. B **232**, 109 (1984).
- [50] V. M. Belyaev, V. M. Braun, A. Khodjamirian and R. Ruckl, Phys. Rev. D **51**, 6177 (1995).
- [51] Q. N. Wang, W. Chen, and H. X. Chen, Chin. Phys. C **45**, 093102 (2021).
- [52] H. X. Chen, Y. X. Yan, W. Chen, Phys. Rev. D **106**, 094019 (2022).
- [53] Q. Xin, and Z. G. Wang, Eur. Phys. J. A **58**, 118 (2022).
- [54] S. S. Agaev, K. Azizi and H. Sundu, Turk. J. Phys. **44**, 95 (2020).
- [55] R. L. Workman *et al.* [Particle Data Group], Prog. Theor. Exp. Phys. **2022**, 083C01 (2022).
- [56] S. S. Agaev, K. Azizi and H. Sundu, Phys. Rev. D **93**, 074002 (2016).
- [57] S. S. Agaev, K. Azizi and H. Sundu, Phys. Rev. D **106**, 014025 (2022).
- [58] S. S. Agaev, K. Azizi and H. Sundu, Phys. Rev. D **93**, 114036 (2016).
- [59] V. Lubicz, A. Melis and S. Simula, PoS LATTICE **2016**, 291 (2017).